Trapping States in the Micromaser

M. Weidinger,[1,2] B. T. H. Varcoe,[1] R. Heerlein,[2] and H. Walther[1,2]
[1]*Max-Planck-Institut für Quantenoptik, 85748 Garching, Germany*
[2]*Sektion Physik der Universität München, 85748 Garching, Germany*
(Received 16 October 1998)

Trapping states in the one-atom maser or micromaser are predicted by maser theory and are a direct consequence of the quantization of the electromagnetic field. They have been found in our experiment when the inversion of atoms leaving the cavity is observed while the interaction time is scanned. They correspond to quantum states of the atom-cavity system and under certain conditions represent Fock states. The trapping states occur when the atom-field dynamics complete a full evolution (or multiples thereof). Owing to feedback through the maser dynamics, a stabilization of the photon number in the steady state field of the maser cavity is achieved. [S0031-9007(99)09112-7]

PACS numbers: 42.50.Dv, 84.40.Ik

One of the simplest systems in quantum mechanics is a two level atom interacting with a single mode of the electromagnetic field. This problem was first treated theoretically by Jaynes and Cummings [1]. The one-atom maser or micromaser is the experimental realization of this system, as it allows one to study the interaction of a single atom with a single mode of a high Q cavity. Cavity Q factors as high as 3×10^{10}, corresponding to an average lifetime of a photon in the cavity of 0.2 s, have been achieved. The photon lifetime is therefore much longer than the interaction time of an atom with the maser field, being approximately 30–130 μs for a thermal atomic beam. The micromaser field is driven by excited state atoms entering the cavity successively which produces a steady state quantum field [2]. The atoms used in the experiments are rubidium Rydberg atoms pumped by laser excitation into the $63P_{3/2}$ upper maser level. The lower maser level is either the $61D_{5/2}$ or the $61D_{3/2}$ depending on the cavity frequency. The atom field dynamics are observed by measuring the state of atoms leaving the cavity in a state sensitive field ionization detector. The field inside the cavity consists of only one to a few photons; nevertheless, it is possible to study the interaction in great detail. The counting statistics of the pump atoms emerging from the cavity allow one to measure the nonclassical nature of the cavity field [3]. The dynamics of the atom field interaction can be investigated by selecting and varying the velocity and therefore the interaction time of the pump atoms. Sub-Poissonian atom statistics [4], bistability and hysteresis [5], and atom-atom interference [6] have all been measured under suitable experimental conditions; for a review, see Refs. [7,8].

A characteristic pump curve of the micromaser is produced by plotting the average photon number as a function of the pump parameter Θ [9], which is defined as

$$\Theta = \sqrt{N_{\mathrm{ex}}}\,\Omega\, t_{\mathrm{int}}\,. \tag{1}$$

Here t_{int} is the interaction time of atoms with the cavity, N_{ex} is the number of atoms passing through the cavity in a field decay time, and Ω is the atom field coupling constant. At low temperatures of the cavity the number of blackbody photons in the cavity mode is reduced and under this condition, trapping states begin to appear [10]. They occur in the micromaser when the atom field coupling, Ω, and the interaction time, t_{int}, are chosen such that in a cavity field with n_q photons each atom undergoes an integer number, k, of Rabi cycles. This is summarized by the condition

$$\Omega\, t_{\mathrm{int}}\sqrt{n_q + 1} = k\pi\,. \tag{2}$$

When Eq. (2) is fulfilled, each atom undergoes a full Rabi cycle leaving the cavity photon number unchanged after the interaction; hence the photon number is "trapped." This will occur regardless of the atomic pump rate N_{ex}. The trapping state is therefore characterized by the upper bound photon number n_q and the number of integer multiples of full Rabi cycles k. Trapping states are quantum features of the micromaser field that occur through the influence of Fock or number states of the electromagnetic field. Related systems making use of single atom dynamics could also display the same features [11].

The preparation of trapping states in the micromaser is of interest as it is a forerunner to the realization of Fock states of an electromagnetic field in steady state [12]. The problems associated with the detection of a trapping state in the micromaser field were discussed in Ref. [7]. Briefly, the Q of the cavity must be high enough that an emitted photon is stored for a period longer than the interaction time and the average atom-atom separation. The atomic lifetime must be long enough that spontaneous emission does not significantly affect the visibility of trapping states in a measurement of atomic statistics. A lower atomic pump rate is preferable to increase the visibility of trapping states by reducing the impact of external fluctuations and two atom effects [13]. The temperature of the cavity must be low enough to remove the influence of thermal photons which prevents perfect inversion even at the positions of trapping states. Finally the atomic beam must have a narrow velocity distribution.

In this paper we report on the first measurements of trapping states in the micromaser. We are able to find interaction times in steady state operation of the micromaser for which the atoms undergo integral numbers of Rabi cycles leaving the cavity photon number unchanged.

The experimental apparatus is presented in Fig. 1 and has been described in detail previously [5]. Briefly, in this experiment, a ^{3}He-^{4}He dilution refrigerator houses the microwave cavity which is a closed superconducting niobium cavity with a quality factor of 1.5×10^{10}. A rubidium oven provides two collimated atomic beams: a central atomic beam passing directly into the cryostat and a second beam directed to an additional excitation region. The second beam was used as a frequency reference. A frequency doubled dye laser ($\lambda = 294$ nm) was used to excite rubidium (^{85}Rb) atoms to the Rydberg $63P_{3/2}$ state from the $5S_{1/2}(F = 3)$ ground state.

Velocity selection is provided by angling the excitation laser towards the main atomic beam at 11° to the normal. The dye laser was locked, using an external computer control, to the $5S_{1/2}(F = 3)$-$63P_{3/2}$ transition of the reference atomic beam excited under normal incidence. The reference transition was detuned by Stark shifting the resonance frequency using a stabilized power supply. This enabled the laser to be tuned while remaining locked to an atomic transition. Figure 2 shows the Doppler broadened spectrum of the velocity selecting laser and the positions of the Stark shifted reference resonance over a range of electric field strengths. The higher peak (indicated) was used as the reference excitation. The measurements of frequency detuning were calibrated using the known fine structure splitting of the 63 Rydberg state at zero electric field. To check this calibration, the polarizability of the $63P_{3/2}$ state was calculated, using our data, to be 1.16 ± 0.04 GHz/(V/cm)^2, compared with a published value of 1.12 GHz/(V/cm)^2 [14]. Time of flight measurements were additionally used to calibrate the velocity of the atoms over a broad range of Stark voltages and using these self-consistent checks the interaction time (t_{int}) was extracted. The velocity width of the selected atomic beam was better than 3%. The interaction time tuning range extended from 30 to 130 μs depending on the available laser power and the desired atomic beam flux. There was an uncertainty in the calculated interaction time of 2 μs, arising from the determination of the cavity length and Stark detunings. For interaction times below 40 μs the Doppler distributions of the $63P_{1/2}$ and $63P_{3/2}$ levels overlap leading to excitation of noninteracting $63P_{1/2}$ atoms disturbing the maser statistics.

The microwave cavity was tuned to the $63P_{3/2}$-$61D_{5/2}$(21.4560 MHz) Rydberg transition in rubidium with a coupling constant $\Omega = 39 \pm 5$ kHz. The lifetimes of the two atomic states are 488 μs and 244 μs, respectively. The coupling constant Ω was determined by calibrating the shape of the maserline for this cavity using a known pump rate, N_{ex}, and interaction time, t_{int}, against theory [6]. When performing an experiment, the data collection program writes a file which records the state (excited or ground) of every detected atom and its arrival time at the state selective detector. Exactly 6400

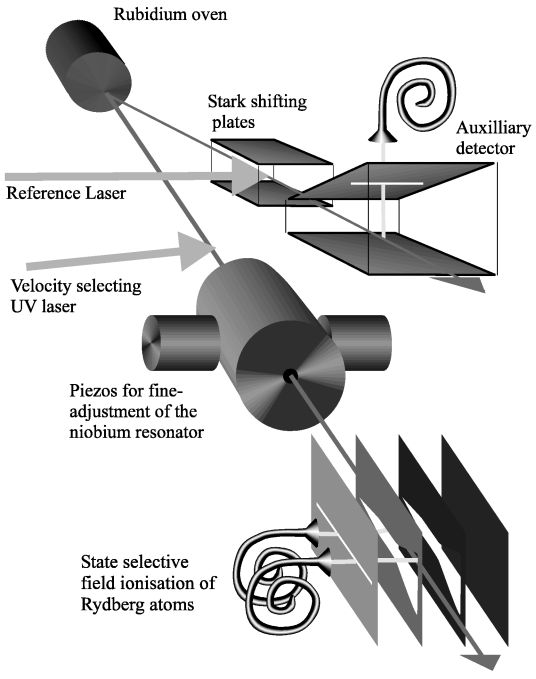

FIG. 1. The experimental setup. The atoms leaving the rubidium oven are excited into the $63P_{3/2}$ Rydberg state using a UV laser at an angle of 11°. Following the cavity the atoms are detected using state selective field ionization. Tuning of the cavity is performed using two piezo translators. The reference beam is used to stabilize the laser frequency to a Stark shifted atomic resonance, allowing the velocity of the atoms to be tuned continuously.

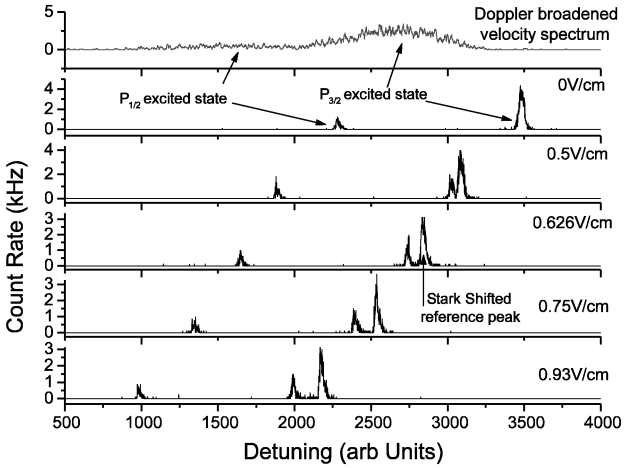

FIG. 2. Position of the $5S_{1/2}$-$63P_{3/2}$ transition as a function of the applied electrical field in the reference unit. The uppermost plot shows the Doppler broadened excitation spectrum of the atoms in the cryostat. It is clearly visible that the laser can be tuned through the velocity distribution while keeping the frequency locked to the indicated peak.

events were logged for every condition of interaction time and pump rate. Using atoms with a $t_{\rm int}$ of 45 μs we determined the overall detection efficiency to be 40% by identifying maser thresholds. Each detector has miscounts of approximately 2%; however, for slower atoms the total detector efficiency is reduced by atomic decay.

When a trapping state is realized by choosing a proper interaction time, the photon number distribution is strongly peaked in the range $n \leq n_q$, in which state the maser remains until a random event occurs, which changes the photon number in the cavity and violates the trapping state condition. In general during the steady state operation of a micromaser in a trapping state, the waiting time between two atoms in the lower state becomes longer and one should expect a general suppression of events in the lower state atom detector and an increase in the upper state detector [15], a feature that should be preserved through increasing atomic pump rate $N_{\rm ex}$. The relevant quantity here is the atomic inversion, I, which is defined as

$$I(t_{\rm int}) = P_g(t_{\rm int}) - P_e(t_{\rm int}), \tag{3}$$

where $P_{e(g)}(t_{\rm int})$ is the probability of finding an excited state (ground state) atom for a particular interaction time $t_{\rm int}$.

A Fock state shows ideal sub-Poissonian statistics. Consequently under the influence of a trapping state the atomic statistics should also be sub-Poissonian. Therefore an independent check of the data is to look at the statistical properties of the emergent atoms, namely, by observing the normalized variance of atoms in the lower state [4,16]. As an atom in the ground state must have emitted a photon into the cavity, the lower state atom statistics are strongly related to cavity photon statistics [3]. Briefly, when the maser is under the influence of a trapping state, an atom cannot emit into the cavity until a photon decays from the mode. When this occurs the next excited state atom entering the cavity will emit a photon with a high probability, returning the cavity to the trapping state. This results in a regular spacing of ground state atoms and a reduction of fluctuations in the count rate. Outside of the trapping state conditions the cavity photon number can take any allowed quantity. Hence, outside of the trapping state condition, a greater level of fluctuations of lower state atoms is expected. The relevant statistical quantity is the Fano-Mandel Q function which indicates the deviation of the counting statistics from Poissonian statistics. It is defined as

$$Q(t) = \frac{\langle n(t)^2\rangle - \langle n(t)\rangle^2}{\langle n(t)\rangle} - 1, \tag{4}$$

where $n(t)$ is the number of counts in an interval of length t. For a Poissonian beam $Q(t) = 0$, sub-Poissonian (reduced fluctuation) statistics produce $Q(t) < 0$ and super-Poissonian (increased fluctuation) statistics produce $Q(t) > 0$.

Figures 3(A) and 3(B) present experimental measurements of the atomic inversion as a function of interaction time for two values of $N_{\rm ex}$ and a cavity temperature of 0.3 K which corresponds to a thermal photon number of 0.054. A linear trend towards longer interaction times can be seen in Figs. 3(A) and 3(B). This occurs as a result of the shorter lifetime of lower state atoms compared to upper state atoms, causing greater loss at long interaction times, which means long flight times to the detector. To apply a first order correction for this effect, the linear trend has been subtracted in Figs. 3(α) and 3(β) to remove the influence of the lifetime effect on the relative visibility of the dips in the curves. This result shows a good qualitative agreement with the Monte Carlo simulations performed in Ref. [7].

In Fig. 3(α) for a lower $N_{\rm ex}$ the trapping states due to the vacuum $[(n_q, k) = (0, 1)]$, one photon $[(n_q, k) = (1, 1)]$, and two photon $[(n_q, k) = (2, 1), (2, 2)]$ trapping states are quite clear, while in Fig. 3(β) the vacuum and one photon trapping state have become less visible. As the pump rate $N_{\rm ex}$ increases, the width of the trapping states decreases [10] and detuning and velocity averaging

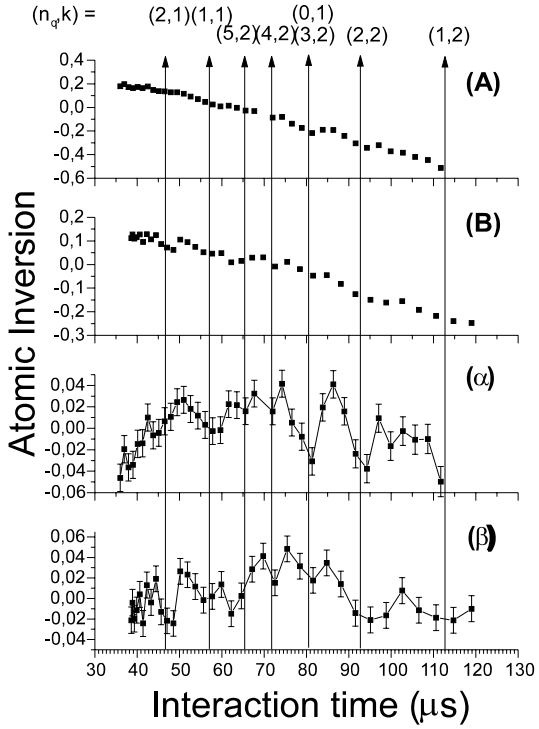

FIG. 3. Atomic inversion as a function of interaction time. Plots (A) and (B) present the inversion as a function of interaction time for pump rates of $N_{\rm ex} = 7$ and $N_{\rm ex} = 10$, respectively. Plots (α) and (β) represent the plots (A) and (B), respectively, after the linear trend was removed (see text). The vertical lines on the plot indicate the theoretical positions of all low order trapping states over the range of interaction times of the plot. Dips in the inversion can be identified as corresponding with the positions of the indicated trapping states. The visibility of trapping states falls with a higher pump rate $N_{\rm ex}$.

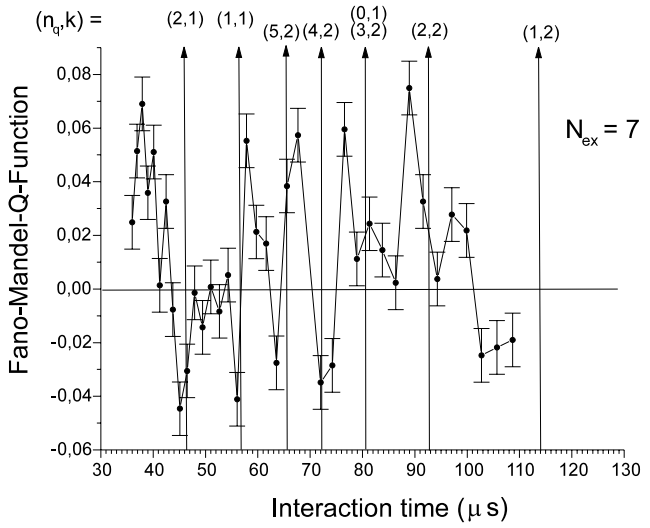

FIG. 4. Fano-Mandel Q function vs interaction time. Suppression of fluctuations can be seen at many indicated positions of trapping states. The error bars are derived from a pessimistic evaluation of the statistical errors of the calculation. We explicitly state that there is an error of 2 μs in the experimental determination of the interaction time. Also owing to a small error in our knowledge of the coupling constant Ω, there is a corresponding uncertainty in the theoretical positions of the trapping states.

have a larger effect. More importantly for higher pump rates the proportion of two atom events grows, reducing the visibility of trapping states. This is an effect that is well documented [13]. The higher visibility using a lower pump rate was therefore expected. For this reason only the lower pump rate curve [Fig. 3(A)] is considered for further analysis.

The Q function of ground state atoms is presented in Fig. 4. Unlike the inversion plots no lifetime modifications were necessary for this graph. To remove excess experimental noise from the data, each point is averaged over time periods between one and four cavity decay times. In sub-Poissonian regions the Q function reaches a steady state value in less than one cavity decay time [3].

In Fig. 4 the effect of trapping states can be seen in the form of reduced fluctuations in the atomic statistics in agreement with the inversion plot Fig. 3(α). When the maser is under the conditions of a vacuum trapping state, the atomic statistic is nearly Poissonian ($Q \simeq 0$). This is to be expected, considering that under the conditions of a vacuum trapping state any emission into the cavity violates the trapping condition [Eq. (2)]. Such events are identified by the detection of a ground state atom and should be randomly distributed. For the higher order trapping states (e.g., for $n_q = 2$) this situation changes. To preserve the trapping condition cavity photons have to be replaced when they are removed from the cavity by the field damping. Consequently there have to be regularly spaced emission events resulting in a reduced fluctuation of the lower state counts on a time scale of about one cavity decay time.

In this paper we report on the first measurements of trapping states in the steady state micromaser field. Two methods of analysis have been applied to the data, an inversion measurement which relies only on the preservation of a steady state field in the micromaser cavity and a statistical approach where the time spacing of the emerging ground state atoms is considered. Both methods reveal an effect on the steady state dynamics of the maser that is due to the influence of trapping states. This work leads the way to future experiments to prepare higher order Fock states and macroscopic superpositions of the field. Using a known interaction time one can readily prepare states of zero, one, two, or more photons in the field. We have shown that the preparation of such states poses no in-principle difficulty for the current micromaser experimental apparatus.

[1] E. T. Jaynes and F. W. Cummings, Proc. IEEE **51**, 89 (1963).
[2] D. Meschede, H. Walther, and G. Müller, Phys. Rev. Lett. **54**, 551 (1985).
[3] H.-J. Briegel *et al.*, Phys. Rev. A **49**, 2962 (1994); G. Rempe, F. Schmidt-Kaler, and H. Walther, Phys. Rev. Lett. **64**, 2783 (1990).
[4] G. Rempe and H. Walther, Phys. Rev. A **42**, 1650 (1990).
[5] O. Benson, G. Raithel, and H. Walther, Phys. Rev. Lett. **72**, 3506 (1994).
[6] G. Raithel, O. Benson, and H. Walther, Phys. Rev. Lett. **75**, 3446 (1995).
[7] G. Raithel *et al.*, in *Advances in Atomic, Molecular and Optical Physics,* edited by P. Berman (Academic Press, New York, 1994), Suppl. 2.
[8] S. Haroche, M. Brune, and J. M. Raimond, Philos. Trans. R. Soc. London A **355**, 2367 (1997).
[9] P. Filipowicz, J. Javanainen, and P. Meystre, Phys. Rev. A **34**, 3077 (1986).
[10] P. Meystre, G. Rempe, and H. Walther, Opt. Lett. **13**, 1078 (1988).
[11] K. An *et al.*, Phys. Rev. Lett. **73**, 3375 (1994).
[12] J. J. Slosser, P. Meystre, and E. M. Wright, Opt. Lett. **15**, 233 (1990).
[13] E. Wehner *et al.*, Opt. Commun. **110**, 655 (1994); M. Orszag *et al.*, Phys. Rev. A **49**, 2933 (1994).
[14] S. Liberman and J. Pinard, Phys. Rev. A **20**, 507 (1979).
[15] C. Wagner, A. Schenzle, and H. Walther, Opt. Commun. **107**, 318 (1994).
[16] D. Meschede and A. Schenzle, in *Atomic, Molecular and Optical Physics Handbook,* edited by G. W. F. Drake (AIP, New York, 1996).